Three dimensional live cell lithography

Anna Linnenberger,[1] Martha I. Bodine,[1] Callie Fiedler,[1] Justine J. Roberts,[2] Stacey C. Skaalure,[2] Joseph P. Quinn,[4] Stephanie J. Bryant,[2,3] Michael Cole,[1] and Robert R. McLeod[1,*]

[1]*Department of Electrical, Computer, and Energy Engineering, University of Colorado, 1111 Engineering Drive, 422 UCB, Boulder, Colorado 80309-0422, USA*

[2]*Department of Chemical and Biological Engineering, University of Colorado, 596 UCB Boulder, Colorado 80309-0596, USA*

[3]*Biofrontiers Institute, University of Colorado, 3415 Colorado Ave, Boulder, Colorado 80303, USA*

[4]*Department of Chemical and Biomolecular Engineering, Rice University, 6100 Main Street, Houston, Texas 77005 USA*

**mcleod@colorado.edu*

Abstract: We investigate holographic optical trapping combined with step-and-repeat maskless projection stereolithography for fine control of 3D position of living cells within a 3D microstructured hydrogel. C2C12 myoblast cells were chosen as a demonstration platform since their development into multinucleated myotubes requires linear arrangements of myoblasts. C2C12 cells are positioned in the monomer solution with multiple optical traps at 1064 nm and then encapsulated by photopolymerization of monomer via projection of a 512x512 spatial light modulator illuminated at 405 nm. High 405 nm sensitivity and complete insensitivity to 1064 nm was enabled by a lithium acylphosphinate (LAP) salt photoinitiator. These wavelengths, in addition to brightfield imaging with a white light LED, could be simultaneously focused by a single oil immersion objective. Large lateral dimensions of the patterned gel/cell structure are achieved by *x* and *y* step-and-repeat process. Large thickness is achieved through multi-layer stereolithography, allowing fabrication of precisely-arranged 3D live cell scaffolds with micron-scale structure and millimeter dimensions. Cells are shown to retain viability after the trapping and encapsulation procedure.

OCIS codes: (350.4855) Optical tweezers or optical manipulation; (220.3740) Lithography; (170.1420) Biology

References and links

1. C. D. James, R. Davis, M. Meyer, A. Turner, S. Turner, G. Withers, L. Kam, G. Banker, H. Craighead, M. Isaacson, J. Turner, and W. Shain, "Aligned microcontact printing of micrometer-scale poly-L-lysine structures for controlled growth of cultured neurons on planar microelectrode arrays," IEEE Trans. Biomed. Eng. **47**(1), 17–21 (2000).
2. S. B. Jun, M. R. Hynd, N. Dowell-Mesfin, K. L. Smith, J. N. Turner, W. Shain, and S. J. Kim, "Low-density neuronal networks cultured using patterned poly-l-lysine on microelectrode arrays," J. Neurosci. Methods **160**(2), 317–326 (2007).
3. D. W. Branch, B. C. Wheeler, G. J. Brewer, and D. E. Leckband, "Long-term maintenance of patterns of hippocampal pyramidal cells on substrates of polyethylene glycol and microstamped polylysine," IEEE Trans. Biomed. Eng. **47**(3), 290–300 (2000).
4. V. L. Tsang and S. N. Bhatia, "Three-dimensional tissue fabrication," Adv. Drug Deliv. Rev. **56**(11), 1635–1647 (2004).
5. U. Mirsaidov, J. Scrimgeour, W. Timp, K. Beck, M. Mir, P. Matsudaira, and G. Timp, "Live cell lithography: using optical tweezers to create synthetic tissue," Lab Chip **8**(12), 2174–2181 (2008).
6. G. Sinclair, P. Jordan, J. Leach, M. J. Padgett, and J. Cooper, "Defining the trapping limits of holographical optical tweezers," J. Mod. Opt. **51**(3), 409–414 (2004).
7. K. T. Nguyen and J. L. West, "Photopolymerizable hydrogels for tissue engineering applications," Biomaterials **23**(22), 4307–4314 (2002).

#185478 - $15.00 USD Received 19 Feb 2013; revised 4 Apr 2013; accepted 6 Apr 2013; published 18 Apr 2013

8. D. Preece, R. Bowman, A. Linnenberger, G. Gibson, S. Serati, and M. Padgett, "Increasing trap stiffness with position clamping in holographic optical tweezers," Opt. Express **17**(25), 22718–22725 (2009).
9. G. M. Gibson, R. W. Bowman, A. Linnenberger, M. Dienerowitz, D. B. Phillips, D. M. Carberry, M. J. Miles, and M. J. Padgett, "A compact holographic optical tweezers instrument," Rev. Sci. Instrum. **83**(11), 113107 (2012).
10. J. Liesener, M. Reicherter, T. Haist, and H. J. Tiziani, "Multi-functional optical tweezers using computer-generated holograms," Opt. Commun. **185**(1-3), 77–82 (2000).
11. G. Sinclair, J. Leach, P. Jordan, G. Gibson, E. Yao, Z. Laczik, M. Padgett, and J. Courtial, "Interactive application in holographic optical tweezers of a multi-plane Gerchberg-Saxton algorithm for three-dimensional light shaping," Opt. Express **12**(8), 1665–1670 (2004).
12. S. J. Bryant, C. R. Nuttelman, and K. S. Anseth, "Cytocompatibility of UV and visible light photoinitiating systems on cultured NIH/3T3 fibroblasts in vitro," J. Biomat. Sci. Polym. E. **11**(5), 439–457 (2000).
13. H. Liang, K. T. Vu, P. Krishnan, T. C. Trang, D. Shin, S. Kimel, and M. W. Berns, "Wavelength dependence of cell cloning efficiency after optical trapping," Biophys. J. **70**(3), 1529–1533 (1996).
14. C. Sun, N. Fang, D. M. Wu, and X. Zhang, "Projection micro-stereolithography using digital micro-mirror dynamic mask," Sens. Actuat. A. **121**, 113–120 (2005).
15. R. Gauvin, Y. C. Chen, J. W. Lee, P. Soman, P. Zorlutuna, J. W. Nichol, H. Bae, S. Chen, and A. Khademhosseini, "Microfabrication of complex porous tissue engineering scaffolds using 3D projection stereolithography," Biomaterials **33**(15), 3824–3834 (2012).
16. B. D. Fairbanks, M. P. Schwartz, C. N. Bowman, and K. S. Anseth, "Photoinitiated polymerization of PEG-diacrylate with lithium phenyl-2,4,6-trimethylbenzoylphosphinate: polymerization rate and cytocompatibility," Biomaterials **30**(35), 6702–6707 (2009).
17. A. S. Sawhney, C. P. Pathak, and J. A. Hubbell, "Bioerodible hydrogels based on photopolymerized poly (ethylene glycol)-co-poly (. alpha.-hydroxy acid) diacrylate macromers," Macromolecules **26**(4), 581–587 (1993).
18. S. J. Bryant, C. R. Nuttelman, and K. S. Anseth, "Cytocompatibility of UV and visible light photoinitiating systems on cultured NIH/3T3 fibroblasts in vitro," J. Biomat. Sci. Polym. E. **11**, 439–457 (2000).
19. C. G. Williams, A. N. Malik, T. K. Kim, P. N. Manson, and J. H. Elisseeff, "Variable cytocompatibility of six cell lines with photoinitiators used for polymerizing hydrogels and cell encapsulation," Biomaterials **26**(11), 1211–1218 (2005).
20. N. E. Fedorovich, M. H. Oudshoorn, D. van Geemen, W. E. Hennink, J. Alblas, and W. J. A. Dhert, "The effect of photopolymerization on stem cells embedded in hydrogels," Biomaterials **30**(3), 344–353 (2009).
21. A. C. Urness, M. C. Cole, K. K. Kamysiak, E. R. Moore, and R. R. McLeod "Liquid deposition photolithography for submicrometer resolution three-dimensional index structuring with large throughput," Light Sci. Appl. **2** (2013).
22. E. Eriksson, J. Scrimgeour, A. Graneli, K. Ramser, R. Wellander, J. Enger, D. Hanstorp, and M. Goksör, "Optical manipulation and microfluidics for studies of single cell dynamics," J. Opt. A, Pure Appl. Opt. **9**(8), S113–S121 (2007).

1. Introduction

Crosslinked polymers are often utilized to create synthetic hydrogel scaffolds for tissue engineering by encapsulating living cells whose development is studied to answer fundamental biological questions and to fabricate regenerative medical implants. Current approaches for fabricating these hydrogel constructs do not provide simultaneous 3D control of polymer structure and 3D placement of cells. 2D patterning of cells is commonly accomplished by lithographic deposition of an extra-cellular protein, for example poly-L-lysine is used to direct neuronal cell attachment and growth on planar electrode arrays [1–3]. Unfortunately, 2D structures do not accurately represent living tissue and thus are not appropriate for many basic biological studies or tissue engineering therapies. As a result, a variety of methods to construct complex 3D tissue scaffolds are under study, most derived from 3D printing [4]. While these methods result in 3D structures that define scaffold shape, they provide no control over the internal distribution of cells within the scaffold. The random distribution of cells limits the repeatability of studies and makes precise experiments involving cell-cell interaction impossible in a 3D scaffold environment. Alternatively, optical trapping has been used to precisely arrange living bacteria in a polymerizable solution [5]. However, the depth of a high-NA optical trapping system is limited by aberrations [6] to approximately ± 20 μm and thus does not provide true 3D structuring of cells.

In this article, we investigate the use of holographic optical trapping, to precisely arrange cells within layers, in combination with projection stereolithography, to fabricate multilayered

#185478 - $15.00 USD Received 19 Feb 2013; revised 4 Apr 2013; accepted 6 Apr 2013; published 18 Apr 2013

3D structures encapsulating these cells. Cells are first arranged by optical traps in a liquid monomer mixture which is then locally crosslinked into a hydrogel by photopolymerization to permanently entrap the cells. The sample is translated laterally and the process is repeated to pattern arbitrarily large *x,y* dimensions. The finished layer is then moved away from the cover slip, causing inflow of the fresh cells and monomer which will be formed into the next layer. *Live cell lithography* [5] thus provides micron-scale 3D control of both cellular distribution and gel structure to enable new forms of engineered 3D live cell tissue scaffolds [7].

To illustrate the potential of this approach for complex 3D structuring of micron-scale objects within a hydrogel, we first demonstrate arrangement of silica beads encapsulated in multiple depth layers and multiple lateral steps. To further demonstrate applicability to cellular biology, we structure C2C12 skeletal myoblasts in biologically relevant patterns including a multi-layer hydrogel with linear arrangements of viable C2C12 cells. This work provides a foundation for future studies of myotube formation via cellular junctions, and eventually formation of complex hierarchical tissue structures.

2. Experimental implementation

High-speed automated holographic optical trapping (HOT) [8] at 1064 nm is used to organize cells in a liquid mixture of cell culture medium, monomer and photoinitiator. The latter two components are utilized to create structured hydrogel by photopolymerization at 405 nm. The LAP photoinitiator was chosen because it displays high 405 nm sensitivity and thus lower photo-toxicity than commonly-used 365 nm but immeasurable response to the extremely intense 1064 trapping wavelength. The additive manufacturing system is built around a commercial holographic optical trapping instrument, Fig. 1, which is modified in two ways. First, a 405 nm patterning system is added to enable hydrogel structuring. Second, a small stereolithography chamber is built into the sample area to enable multi-layer fabrication. This 3D printing apparatus is held on precision *x,y* stages, enabling large lateral area via a step-and-repeat processes.

2.1 Holographic optical tweezers

A diagram of the Cube (Boulder Nonlinear Systems) holographic trapping instrument is shown in Fig. 2 [9]. Diffraction limited optical traps are formed using a 10 watt 1064 nm fiber laser (IPG Photonics, YLR-5-1064-LP) which illuminates a mirrored 512x512 pixel phase-only liquid crystal spatial light modulator (P512-1064 SLM, Boulder Nonlinear Systems) through a Keplerian beam expander. The phase patterns on the SLM are computed using the Lenses and Gratings algorithm [10, 11] programmed in OpenGL and running on a graphics co-processor (nVidia Quadro FX 5600). The SLM is imaged to the back aperture of the 1.35 NA oil immersion microscope objective (Olympus UAPON 40XO340) through a 4F imaging system. The objective has at least 65% transmission from 405 nm to 1064 nm, making it possible to simultaneously optically trap, image, and photopolymerize the sample. This system is capable of simultaneously trapping up to 400 objects within a volume with depth limited by aberrations to approximately ± 20μm [5] without time sharing, in addition to correcting for aberrations as a result of the SLM and optical train [9].

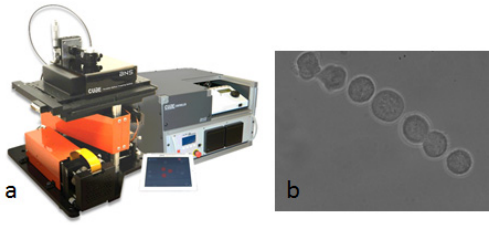

Fig. 1. (a) Cube (Boulder Nonlinear Systems) (b) sample image of 7 optically trapped C2C12 cells.

#185478 - $15.00 USD Received 19 Feb 2013; revised 4 Apr 2013; accepted 6 Apr 2013; published 18 Apr 2013

2.2 Maskless projection lithography

A 410 mW, 405 nm LED (Thorlabs M405L2) is used as the light source to provide spatially uniform illumination with low coherence to suppress speckle noise and interference. The LED is polarized and used to illuminate a 512x512 pixel liquid crystal SLM (Boulder Nonlinear Systems P512-532) employed as a programmable amplitude mask. In contrast to the SLM used for trapping, the linear polarization incident upon this SLM is oriented at 45 degrees relative to the liquid crystal director, resulting in a pixilated programmable polarization rotation. This polarization rotation is converted to amplitude modulation by an orthogonal polarizer. These crossed polarizers prevent unwanted reflections off of surfaces of the SLM from degrading the quality of the off state, resulting in a contrast ratio of 200:1 or better. Use of a chrome mask or a digital micromirror array would result in a higher contrast ratio, but for this application the contrast ratio of the SLM was sufficient. A dichroic mirror (NT69-201, Edmund Optics) is used to introduce the 405 nm pattern into the imaging arm of the Cube, as shown in Fig. 2, such that the SLM plane is in focus at the sample.

This system is capable of photopolymerizing hydrogel patterns with approximately 10 μm resolution in 3-5 seconds using a sample plane intensity of approximately 70 mW/cm^2, which is within the range of other work demonstrating cytocompatibility [12]. This resolution is material-limited due to the balance of the polymerization reaction and the diffusion of photo-generated species in the initially liquid solution. We note that, unlike the 1064 nm trapping pathway, possible aberrations of the 405 nm optical imaging path were not measured or corrected because polymer feature resolution at the diffraction limit is not required for creating structures matching cellular resolution. A critical feature of the gelation process is that it must not perturb the position of objects held in the 1064 nm traps. High intensity in a single spot, such as that from a focused 405 nm laser, gels the polymer more quickly but completely disrupts the positions of trapped objects as polymerization shrinkage and diffusional mass transport overcome the approximately pN trap strength.

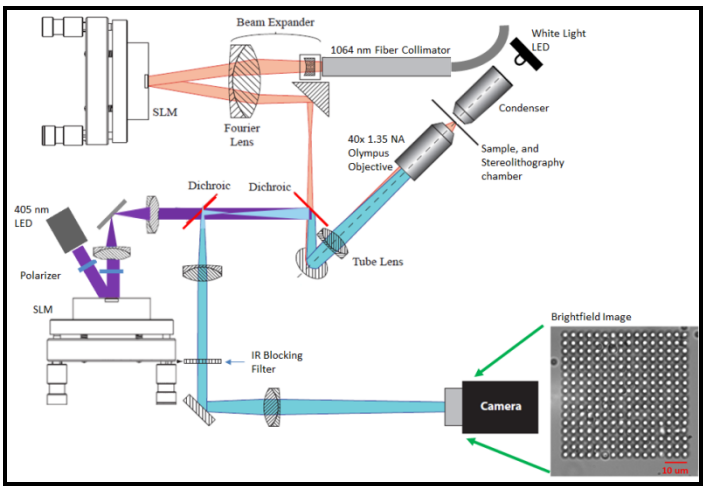

Fig. 2. Optical layout of the Cube modified to include the 405 nm curing system. Sample image contains 256 optically trapped 2 um silica beads in water.

Patterning resolution and trap stability during polymerization is illustrated via "step-and-repeat" structuring shown in Fig. 3. In each of the four sequential exposures, 2μm silica beads are first positioned within the liquid solution by the 1064 nm trapping system. The trapped beads are then illuminated at 405 nm in a 6 × 6 micron square from 9 × 9 SLM pixels, transforming the liquid to a gel without disturbing the trapped objects. Automated stages move the sample to the left and the process is repeated. Although the solid hydrogel cannot be distinguished from the liquid solution in this brightfield image (or even in differential

#185478 - $15.00 USD Received 19 Feb 2013; revised 4 Apr 2013; accepted 6 Apr 2013; published 18 Apr 2013

interference contrast microscopy (DIC) due to the weak index change) the localized solidification is demonstrated by the immediate immobility of the trapped beads and the continued mobility of nearby beads used in the subsequent steps. Use of other techniques to evaluate the shape of the polymer voxel will the one topic addressed in future research. This localized gelation has three benefits. First, 1064 nm dose (which is typically toxic beyond approximately 1 GJ/cm^2 [13]) can be minimized by locally encapsulating cells as soon as they are correctly positioned. Second, the lateral size of the structure is no longer limited to the 345 μm x 345 μm area covered by the SLM but instead can be as large as the motion range of the stages holding the sample, which is 100 mm x100 mm in the Cube system. Finally, the ability to pattern the gel within an arbitrarily-large, single layer can be combined with a multi-layer printing technique to create 3D shapes of mm-dimensions as described next.

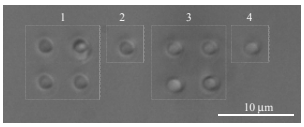

Fig. 3. Brightfield image from the Cube imaging path after four sequential "step and repeat" patterning steps. In each exposure, the 2 μm beads are first trapped at 1064 nm, then the surrounding liquid is locally gelled using 405 nm light controlled by the SLM. The material patterning resolution is demonstrated by the bead spacing while the stability of the traps during gelation is demonstrated by the regular grid.

2.3 Stereolithography

Large 3D scaffolds containing precisely positioned cells can be built from many individual layers through additive manufacturing. In traditional stereolithography [14], photopolymerized structures are formed in a thin monomer layer spread onto the top of the part by a blade. An alternative which removes the open surface and applicator blade is to hold the thin monomer layer between the part and an optical window whose inner surface has been coated to prevent adhesion of polymer [15]. As we show in Fig. 4 and Fig. 5, this approach has the particular advantage that the entire device can be miniaturized sufficiently to fit into the slide holder of an *x,y* motorized microscope stage. The lower surface is a standard cover slip whose upper surface is silane coated to prevent bonding of monomer during polymerization. The objective working distance enables cells to be trapped and polymerization to be initiated up to 40 μm from the inner surface of the window. The cover slip window is held in a baseplate attached to the *x,y* translation stages (MS-2000-XY, ASI) of the Cube. The top of the fabrication chamber is formed by a microscope slide and a glass spacer treated with a siloxane adhesion promoter. The all-glass construction enables brightfield illumination to enter the chamber from above.

A thin fluid layer is initially formed between the top and bottom windows by adjusting the by *z* actuators (here manual screws, although the design is compatible with miniature motorized actuators). The glass spacer compensates for the mechanical height of the chamber, allowing the first layer to be near zero thickness. After a layer of cells encapsulated in a structured hydrogel is formed, the *z* actuators are used to raise both the upper window and the adhered gel layer, after which the process repeats. The minimum layer thickness of several microns is determined by the actuator resolution and the cell diameter while the maximum sample thickness of several cm is limited by actuator range and the sample volume of the microscope. Individual layer thickness can be optically verified using the motorized *z* autofocus actuator on the objective. The result is a precise arrangement of cells with fine control of 3D position within each layer, and extended 3D position throughout the multi-layer scaffold. Layers with different cell types [5] and cell distributions can be sequentially added to rapidly fabricate complex scaffold geometries precisely loaded with individual cells.

#185478 - $15.00 USD Received 19 Feb 2013; revised 4 Apr 2013; accepted 6 Apr 2013; published 18 Apr 2013

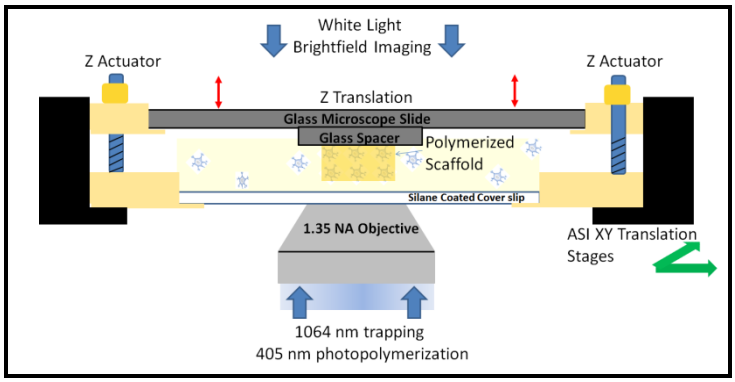

Fig. 4. Side view of the micro stereolithography chamber used for additive lithography of a thick 3D polymer scaffolds. The scaffold is constructed by optically trapping cells, followed by curing of polymer voxels using a 405 nm source. Large lateral dimensions can be fabricated by translating the chamber in x and y to repetition the process. After a layer has been constructed, the upper slide is raised, pulling in new cell-monomer solution and the process is repeated.

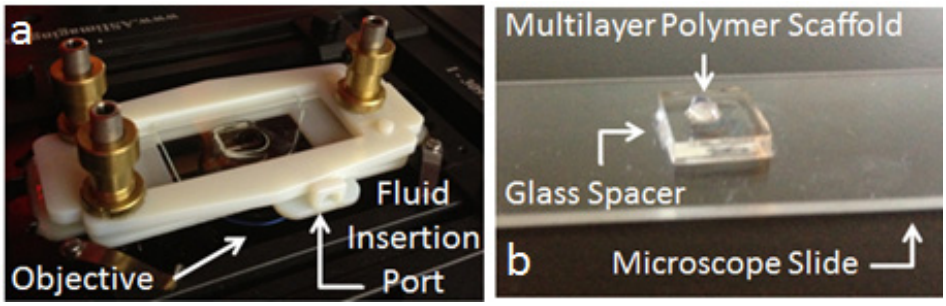

Fig. 5(a) Extrusion system. (b) Microscope slide with the glass spacer and a multi-layer structure of 2 um silica beads in polymer.

2.4 Materials and methods

The cell solution consists of 0.5 million C2C12 (see below) cells/mL suspended in growth media (high glucose Dulbecco's Modified Eagle's Medium containing 10% fetal bovine serum, 1% Penicillin/Streptomyocin, 0.5 µg/mL fungizone). The monomer solution consists of 49.9 wt % phosphate buffered saline (PBS, Cellgro), 0.1 wt % lithium acylphosphinate (LAP) initiator [16], 10 wt % polyethylene glycol dimethacrylate [17] (PEGDA, Sigma), and 40 wt % cell solution. LAP was chosen over initiators commonly used for tissue engineering such as I2959 or eosin [18–20] for several reasons. First, its high water solubility (up to 8.5 wt%) enables photosensitivity to be adjusted over a large range. Second, LAP exhibits low yellowing making it possible to deliver the brightfield illumination through a thick layer of polymerized scaffold without significant absorption. The use of 405 nm, rather than the common 365 nm, reduces cytotoxicity [16] of repeated exposures during multi-layer fabrication and also enables the use of a high-power LED module for faster fabrication. This same choice also significantly relaxes the bandwidth requirements on the microscope objective which must extend up to 1064 nm. Finally, LAP, in the formulation here, did not initiate polymerization in solution when exposed to approximately 0.03 GW/cm^2 of 1064 nm trapping for 10 minutes.

To build multi-layer samples, the photolymerized gel must adhere well to the upper glass spacer but not to the lower coverslip. A methacrylate coating on the glass spacer is used promote adhesion of the polymer voxel to the spacer, while a silane coating prevents adhesion of polymer to the coverslip. An oxygen-rich layer of PDMS has been used to eliminate

#185478 - $15.00 USD Received 19 Feb 2013; revised 4 Apr 2013; accepted 6 Apr 2013; published 18 Apr 2013

adhesion of radical polymerization [21] but it was found that this suppressed polymerization at the working plane of the 1.35 NA objective. The coating is deposited on the coverslip by mixing 0.6 g IPA with 0.017 g acetic acid (A6268, Aldrich) and 0.04 g (heptadecafluoro1.1.2.2-tetra-hydrodecyl) trimethoxy silane (Gelest). The mixture is placed between two coverslips stacked together, and the coverslips are baked on a hot plate at 70 °C for 10 minutes. After baking coverslips are detached from each other, and rinsed with isopropyl alcohol and distilled water. The microscope slide with the transparent glass spacer is similarly coated; however, 3-(triethoxysilyl)propyl methacrylate (Tokyo Chemical Industry) is used in place of (heptadecafluoro1.1.2.2-tetra-hydrodecyl) trimethoxy silane such that the coating promotes adhesion of polymer to the glass spacer.

Structures containing both two micron silica beads (Sekisui) and live cell structures are fabricated. The live cells used here are C2C12 mouse myoblast (ATCC) cultured in growth medium (as above), at 37°C and in 5% CO_2. Upon reaching 70-80% confluency, cells were passaged with 0.25% trypsin, and either re-plated for continued expansion or combined with polymer solution for photoencapsulation (passage ~40). After entrapment within scaffolds, cells were assessed for viability with the LIVE/DEAD® membrane integrity assay, and imaged with a confocal laser scanning microscope (CLSM, Zeiss LSM 510, Thornwood, NY) at 40x magnification.

3. Results and discussion

To illustrate complex 3D structuring, we first show multilayer grids of silica beads encapsulated within the hydrogel. As shown in Fig. 6(a), each layer consists of 2 μm silica beads arranged into a 6x6 bead grid. Spacing between each layer is 95 μm. Lateral registration between the layers is 4 μm, limited by the manual micrometers used here. Figure 6(b) demonstrates the ability to pattern large scale structures in x and y. Grids of 2 μm silica beads are arranged in 3x3 grids, and a supporting polymer voxel approximately 30 μm x 20 μm is used to solidify the arrangement. The sample is translated in x and y 10 times to fabricate a large scale single sheet.

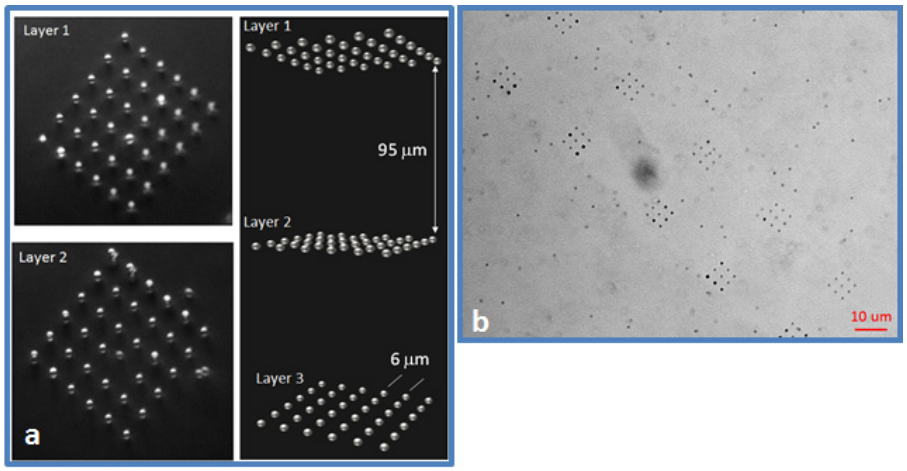

Fig. 6. (a, left) DIC image of a multi-layer grid of 2 μm silica beads, where each layer contained 64 beads organized into a 6x6 bead matrix. (a, right) Rendering of the multi-layer structure showing scale of the arrangement. (b) large scale pattern of 2 μm silica beads organized into 3x3 bead grids which was fabricated through 10 time sequential cures

The fabrication of 3D organized cell-encapsulated scaffolds demonstrates the capability of the system to structure biologically relevant cellular constructs. A two layer structure of C2C12 myoblasts is shown in Fig. 7(a) and Fig. 7(b). The first layer consists of a line of 6 cells. Layer 2 consists of a line of 3 cells, slightly shifted to the side such that the first layer

#185478 - $15.00 USD Received 19 Feb 2013; revised 4 Apr 2013; accepted 6 Apr 2013; published 18 Apr 2013

can still be seen. Figure 7(c) show grids fabricated using a step-and-repeat approach. In each grid a single cell was trapped and encased in a polymer voxel approximately 100 µm x 90 µm in size. The results of Fig. 7(b) highlight a challenge with the approach. It is not always possible to find cells freely floating near to where they are needed. The simple solution is to increase the cell concentration, but this can lead to unwanted cells in the cured polymer, which would negate the purpose of the tool. This has previously been overcome by creating a flow of cells from which cells are selectively removed for use in the fabricated structures [22].

Single layers of organized cells were placed in PBS buffer mixed with 1 µL calcein AM and 2 uL ethidium homodimer to perform a LIVE/DEAD® viability assay. In initial efforts, cells were exposed to traps for up to 5 minutes, resulting in cell death (indicated by red fluorescence in the LIVE/DEAD viability assay). It was found that, consistent with previous work [12], cells optically trapped for 1 – 2 minutes with less than 200 mW per trap (approximately 1.47 GJ/cm^2) were viable. Figure 8 shows linear arrangements of cells that were viable after patterning and curing.

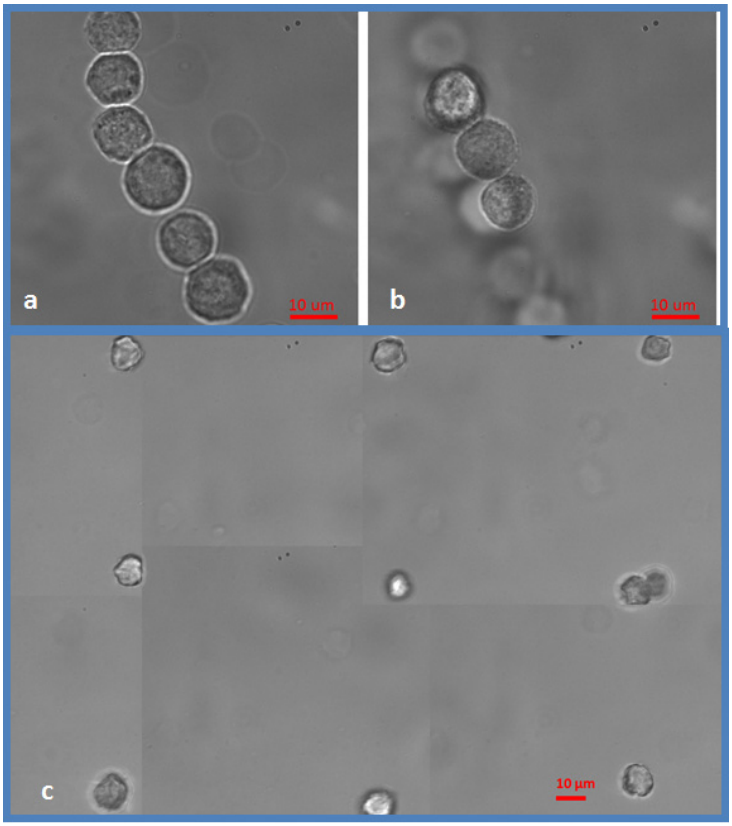

Fig. 7. In all sub-figures scale bars are 10 µm (a) Six C2C12 cells arranged in a line and encapsulated in layer 1 (b) Three trapped cell placed above the line of 6 cells. The slight displacement of the second layer enables an out of focus view of the layer behind. (c) Step and repeat grid fabricated through a series of 9 cures. The images are mosaics of multiple images since the entire structure is larger than the field of view.

#185478 - $15.00 USD Received 19 Feb 2013; revised 4 Apr 2013; accepted 6 Apr 2013; published 18 Apr 2013

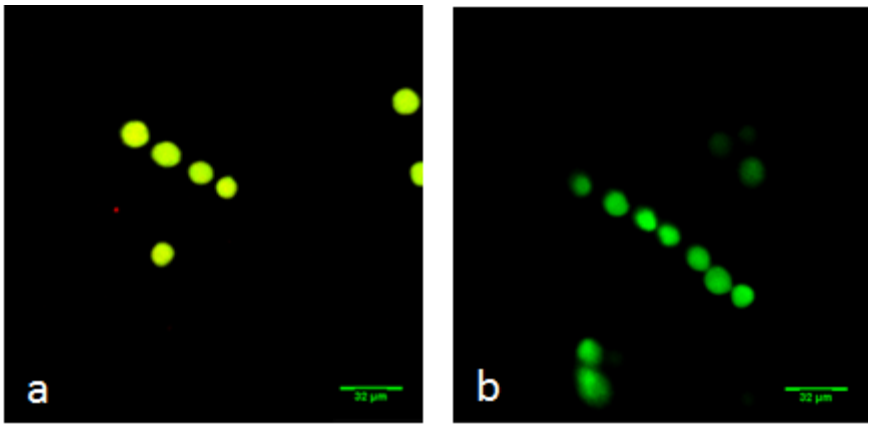

Fig. 8. Viability of arranged lines of C2C12 cells entrapped in polymer scaffold. Green indicates live cells, and red indicates apoptosis

4. Conclusions

We demonstrate a new fabrication method for complex tissue constructs with lithographically-precise cellular arrangement combined with 3D additive lithography of the polymer structure. This is made possible by the incorporation of a miniature stereolithographic printer into a commercial holographic optical trapping instrument. The trapping system can simultaneously manipulate up to 400 objects at 1064 nm without initiating polymerization of the PEGDA monomer. The additive manufacturing system projects images from a 0.25 Mpixel spatial light modulator illuminated at 405 nm through the adhesion-suppressed coverslip to pattern the gel in 2-3 seconds per exposure. Precision *x,y* automated stages enable large lateral structure size, after which micrometers are used to raise the fabrication in *z* for the subsequent layer. The gelation process is shown to preserve the location of trapped objects and ten micron 3D polymer resolution is demonstrated. Multilayer constructs of both beads and viable C2C12 cells are shown with positioning accuracy of approximately one micron. This provides a foundation for rapid fabrication of a new class of 3D tissue construct with cellular-level organization, enabling precise studies of the roll of cellular communication in tissue and cellular development.

Acknowledgments

The authors would like to acknowledge the support of: NSF GOALI (ECCS 0954202), NSF CAREER (ECCS 0847390), Air Force MURI FA9550-09-1-0677, NSF GRFP, NIST MSE Fellowship, and a University of Colorado Innovative Seed Grant, which made this research possible.

#185478 - $15.00 USD Received 19 Feb 2013; revised 4 Apr 2013; accepted 6 Apr 2013; published 18 Apr 2013